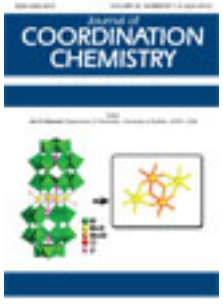

Journal of Coordination Chemistry
Publication details, including instructions for authors and subscription information:
http://www.tandfonline.com/loi/gcoo20

Synthesis and characterization of copper(II) complexes of sulfadiazine with amino acids: catalytic activity toward oxidation of phenol and catechol

Ahmed I. Hanafy [a b], Zeinhom M. El-Bahy [a b] & Ibraheem O. Ali [b]
[a] Chemistry Department, Faculty of Science, Taif University, Taif, Saudi Arabia
[b] Chemistry Department, Faculty of Science, Al-Azhar University, Nasr City, 11884 Cairo, Egypt
Published online: 30 Mar 2012.

To cite this article: Ahmed I. Hanafy, Zeinhom M. El-Bahy & Ibraheem O. Ali (2012) Synthesis and characterization of copper(II) complexes of sulfadiazine with amino acids: catalytic activity toward oxidation of phenol and catechol, Journal of Coordination Chemistry, 65:8, 1459-1474, DOI: 10.1080/00958972.2012.671936

To link to this article: http://dx.doi.org/10.1080/00958972.2012.671936

Journal of Coordination Chemistry
Vol. 65, No. 8, 20 April 2012, 1459–1474

Synthesis and characterization of copper(II) complexes of sulfadiazine with amino acids: catalytic activity toward oxidation of phenol and catechol

AHMED I. HANAFY*†‡, ZEINHOM M. EL-BAHY†‡ and IBRAHEEM O. ALI‡

†Chemistry Department, Faculty of Science, Taif University, Taif, Saudi Arabia
‡Chemistry Department, Faculty of Science, Al-Azhar University, Nasr City, 11884 Cairo, Egypt

(*Received 10 September 2011; in final form 27 January 2012*)

New copper complexes of DL-methioninoylsulfadiazine (MTS) and L-cystinoylsulfadiazine (CYS) were prepared and characterized using elemental analysis, IR, electronic spectroscopy, EPR spectroscopy, and thermal analysis. The mode of binding indicates that copper binds to MTS through carbonyl oxygen with the amino group nitrogen while for Cu^{II}–CYS the copper binds through carbonyl oxygen and SH with removal of its proton. The proposed structures were supported by conformational analysis which showed predominance of the *trans* form of copper(II)-L-cystinoylsulfadiazine. The two complexes enhanced oxidation of phenol and catechol in the presence of H_2O_2 under mild conditions. The catalyst shows proficiency toward oxidation of phenol and catechol compared to the auto-catalytic oxidation. Cu^{II}–MTS exhibited higher catalytic activity than Cu^{II}–CYS. The phenol and catechol oxidation is inhibited by Kojic acid.

Keywords: Sulfadiazine; Amino acids; Oxidation; Phenol; Catechol; Inhibition

1. Introduction

Since environmental and economic factors make the use of harmful oxidants increasingly unacceptable, hydrogen peroxide is used in oxidation of phenolic compounds. Oxidation can be carried out by a large number of natural enzymes that catalyze the oxidation in the presence or absence of oxidant. Catechol oxidases are enzymes that belong to type 3 copper proteins and catalyze only the oxidation of catechols to quinones in the presence of dioxygen [1, 2]. The two other known type 3 copper proteins are hemocyanins and tyrosinases. Hemocyanins, the dioxygen carrier protein in arthropods and mollusks, reversibly bind molecular oxygen. Tyrosinases catalyze both the hydroxylation of phenols to *o*-diphenols (monophenolase activity) and the two-electron oxidation of catechol to quinones (catecholase activity) [3, 4]. There is interest in the catechol oxidase activity of copper complexes using catechol and

*Corresponding author. Email: ahmedih@yahoo.com

ISSN 0095-8972 print/ISSN 1029-0389 online © 2012 Taylor & Francis
http://dx.doi.org/10.1080/00958972.2012.671936

3,5-di-*tert*-butylcatechol as convenient model substrates. Copper complexes serve as functional mimics for catechol oxidases or as new biomimetic catalysts for oxidation reactions [5–10]. In oxidative catalysis, transition metal complexes with polydentate ligands are often used to model structural or functional properties of non-heme enzymes [11]. For catechol oxidation by copper complexes, several mononuclear and dinuclear copper complexes have been studied serving as models for the active sites of copper proteins and the observed biomimetic activity has been correlated with their structural features [12, 13]. The binding and activation of small molecules like dioxygen under mild conditions by enzymatic systems and biomimetic complexes is a very active research field connecting chemical synthesis and catalysis with technology [14, 15].

Herein, we present the synthesis and characterization of simple and safe complexes derived from sulfadiazine and two amino acids. Sulfadiazine and amino acids have been chosen due to the antibacterial activity of sulfadiazine and the ability of the prepared ligands to bind transition metals, mimicking the active site center in natural enzymes. The copper complexes have been used as oxidase synthetic models in phenol and catechol oxidation in the presence of the green oxidizing agent, H_2O_2.

2. Experimental

2.1. *Materials*

Sulfadiazine, DL-methionine, L-cystine, *N*,*N*′-dicyclohexylurea, phenol, catechol, and Fmoc (9*H*-fluoren-9-ylmethoxycarbonyl) were purchased from Sigma-Aldrich. Kojic acid, 3-methyl-2-benzothiazolinone hydrazone (MBTH) and copper chloride were purchased from Merck company.

2.2. *Synthesis of ligands*

A mixture of 0.01 mol of sulfadiazine and 0.01 mol of Fmoc-DL-methionine or Fmoc-L-cystine was dissolved in ~40 mL tetrahydrofuran. The mixture was cooled to 0°C, then 2.06 g (0.01 mol) *N*,*N*′-dicyclohexylcarbodiimide (DCCD) dissolved in ~10 mL tetrahydrofuran was added. The reaction mixture was stirred for 3–5 h at 0°C and allowed to stand for 24 h at room temperature. A few drops of acetic acid and water were added, then the precipitate of *N*,*N*′-dicyclohexylurea was filtered off. The filtrate was concentrated *in vacuo* to dryness. The residual material was recrystallized from ethanol to water and obtained in 80% yield (schemes 1 and 2). The DL-methioninoylsulfadiazine and L-cystinoylsulfadiazine were chromatographically homogeneous when developed with iodine–benzidine solution and gave negative ninhydrin test.

2.2.1. DL-methioninoylsulfadiazine (MTS). IR (KBr); 3348, 3260 cm^{-1} $\nu(NH_2)$, 3100 cm^{-1} ν(NH), 3036 cm^{-1} $\nu(CH\text{-}_{arom.})$, 2936 cm^{-1} $\nu(CH\text{-}_{ali.})$, 1650 cm^{-1} ν(CO), 1586 cm^{-1} ν(CN), 1494 cm^{-1} $\beta(NH_2)$, 1440 cm^{-1} $\nu(SO_2)$; ^{1}H NMR (300 MHz, DMSO) $\delta = 11.11$ (*b*, *s*, 2 H-N$\underline{\mathbf{H}}_2$), 8.47 (s, 2 H, $2CH\text{-}_{pyrimidin}$), 7.96–6.59 (m, 5 H- (4 H, ArH + 1 H), $CH\text{-}_{pyrimidin}$), 5.99 (s, 1 H-N$\underline{\mathbf{H}}SO_2$), 3.386–2.09 (m, 8 $H\text{-}_{aliphatic\ protons}$);

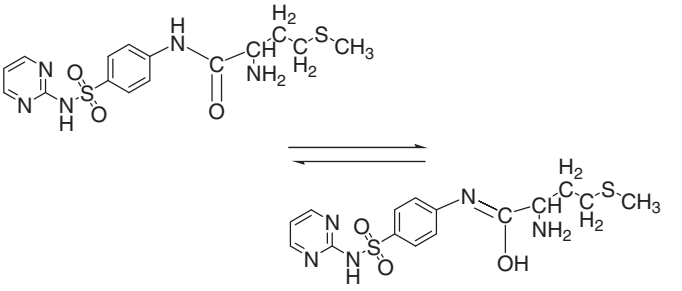

Scheme 1. Tautomeric form of DL-methioninoylsulfadiazine (MTS).

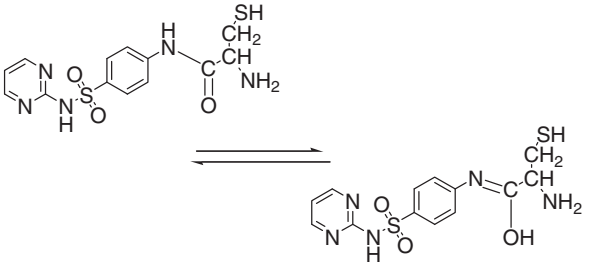

Scheme 2. Tautomeric form of L-cystinoylsulfadiazine (CYS).

Anal./Calcd for $C_{15}H_{19}N_5O_3S_2$ (%): C (47.2); H (4.9); N (18.3). Found: C (47.2); H (5.0); N (18.4).

2.2.2. L-cystinoylsulfadiazine (CYS). IR (KBr); 3380, 3225 cm^{-1} $\nu(NH_2)$, 3036 cm^{-1} ν(NH), 2850 cm^{-1} $\nu(CH\text{-}_{arom.})$, 1650 cm^{-1} ν(CO), 1596 cm^{-1} ν(CN), 1494 cm^{-1} $\beta(NH_2)$, 1440 cm^{-1} $\nu(SO_2)$, 2650 cm^{-1} ν(SH); ^{1}H NMR (300 MHz, DMSO) $\delta = 11.26$(*bs*, 2 H-N**H**$_2$), 8.47(s, 2 H, 2C**H**-$_{pyrimidin}$), 7.96–6.55 (m, 5 H- (4 H, ArH + 1 H), CH-$_{pyrimidin}$), 6.00 (s, 1 H-N**H**SO_2), 2.88 (s, H, C**H**-$_{Cys}$), 2.73 (s, 2 H, C**H**$_2$-$_{Cys}$), 2.08 (s, H, S**H**-$_{Cys}$); Anal./Calcd for $C_{13}H_{15}N_5O_3S_2$ (%): C (44.2); H (4.2); N (19.8). Found: C (44.1); H (4.3); N (19.8).

2.3. Synthesis of copper complexes. Copper(II) chloride (0.01 mol) was dissolved in ~40 mL absolute ethanol, then it was added to 0.01 mol of the prepared ligand dissolved in ~40 mL absolute ethanol. The mixture was heated under reflux for ~2 h. A precipitate formed was filtered off and finally washed with hot ethanol several times.

2.3.1. Cu^{II}-MTS; [CuL(OH)$_2$]. IR (KBr); 3365, 3238 cm^{-1} $\nu(NH_2)$, 3100 cm^{-1} ν(NH), 3037 cm^{-1} $\nu(CH\text{-}_{arom.})$, 2935 $\nu(CH\text{-}_{ali.})$, 1632 cm^{-1} ν(CO), 1586 cm^{-1} ν(CN), 1504 cm^{-1} $\beta(NH_2)$, 1440 cm^{-1} $\nu(SO_2)$; electronic spectrum: $\lambda_{max} = 280$ nm, $\lambda_{max} = 414$ nm, and $\lambda_{max} = 650$ nm. Anal./Calcd for $CuC_{15}H_{20}N_5O_5S_2$ (%): C (37.7); H (4.2); N (15.6); Cu (13.3). Found: C (37.9); H (3.8); N (15.8); Cu (12.8).

2.3.2. Cu^{II}–CYS; $[Cu(L–H)_2 \cdot (H_2O)_2]$. IR (KBr); 3382, 3226 cm^{-1} $\nu(NH_2)$, 3037 cm^{-1} $\nu(NH)$, 2850 cm^{-1} $\nu(CH\text{-}_{arom.})$, 1634 cm^{-1} $\nu(C{=}O)$, 1596 cm^{-1} $\nu(CN)$, 1494 cm^{-1} $\beta(NH_2)$, 1440 cm^{-1} $\nu(SO_2)$; electronic spectrum: $\lambda_{max} = 270$ nm, $\lambda_{max} = 320$ nm, and $\lambda_{max} = 700$ nm. Anal./Calcd for $CuC_{26}H_{32}N_{10}O_8S_4$ (%): C (38.8); H (3.9); N (17.4); Cu (7.9). Found: C (39.4); H (3.9); N (17.5), Cu (8.3).

2.4. *Physical methods*

Carbon, hydrogen, and nitrogen were determined at the Microanalytical Unit, Cairo University, Egypt. Infrared (IR) spectra of the ligands and their solid complexes were measured in KBr on a Mattson 5000 FTIR spectrometer. All electronic spectra and kinetic measurements were performed using a Varian Cary 4 Bio UV-Vis spectrophotometer. ^1H NMR spectra of the ligands were recorded on Joel-90Q Fourier Transform (300 MHz) spectrometers in [D_6] DMSO. Thermal analyses (TGA, DTA) were recorded on a Shimadzu thermo-gravimetric analyzer model TGA-50 H using 20 mg samples. The flow rate of nitrogen and heating rate were 20 $cm^3\,min^{-1}$ and 10°C min^{-1}, respectively. Electron paramagnetic resonance (EPR) spectra were obtained on a Bruker EMX spectrometer working in the X-band (9.78 GHz) with 100 kHz modulation frequency. The microwave power and modulation amplitudes were set at 1 mW. Magnetic susceptibility measurements for the complexes were determined with a Gouy balance using $Hg[Co(NCS)_4]$ as a calibrant at room temperature. The molar conductivities of Cu^{II}–MTS and Cu^{II}–CYS in DMSO were carried out using a TDS model 72 conductivity bridge.

2.5. *Molecular modeling methods*

Conformational analysis: Initial molecular structures of the ligands and complexes were built using the HyperChem program 7.5. Conformational analysis has been performed by use of MM+ [16] force field (calculations *in vacuo*, bond dipole option for electrostatics, Polake Ribiere algorithm, and RMS gradient of 0.01 kcal mol^{-1}). Furthermore, the geometrical optimization with semi-empirical (PM3) molecular orbital method was preformed [17]. The resulting conformations were confirmed as minima by vibrational analysis.

2.6. *Kinetic reactions for phenol and catechol oxidation*

The catalytic activity of Cu^{II}–MTS and Cu^{II}–CYS toward the homogeneous oxidation of phenol and catechol in ethanolic solution at 25°C was determined by measuring the initial rate of oxidation. MBTH was added to copper(II) complex together with very dilute solution of phenol or catechol dissolved in ethanol, then H_2O_2 was added to the solution in a UV-cell to perform the oxidation. The increase of absorption at 500 nm ($\varepsilon = 3.25 \times 10^4$ $(mol\,L^{-1})^{-1}\,cm^{-1}$) due to the formation of adduct between MBTH with the oxidized form of phenol or catechol [18] with time was obtained on a Varian Cary 3 E spectrophotometer. The initial rate was determined from linear increase in concentration with time. To study the effect of the catalyst concentration on the rate of the reaction, various amounts of the complex (40–500 μmol L^{-1}) were used with

$200\,\mu mol\,L^{-1}$ H_2O_2 for oxidation of $1.0\,mmol\,L^{-1}$ phenol or catechol at 25°C; $100\,\mu mol\,L^{-1}$ of copper complex (Cu^{II}–MTS or Cu^{II}–CYS) has been used in the oxidation of different concentrations of the substrate (200–4500 $\mu mol\,L^{-1}$) in the presence of $200\,\mu mol\,L^{-1}$ H_2O_2 to study the effect of phenol or catechol concentration on the reaction. The rate laws were determined and rate constants were obtained. The dependence of H_2O_2 on substrate oxidation by $100\,\mu mol\,L^{-1}$ copper complex was determined by measuring the oxidation rate at different concentrations of hydrogen peroxide (20–400 $\mu mol\,L^{-1}$) in the presence of $1.0\,mol\,L^{-1}$ phenol or catechol in ethanol at 25°C. The auto-oxidation rate of the substrate was determined under the same conditions in the absence of copper complex. Inhibition studies were carried out in a similar fashion as the kinetic measurements using $100\,\mu mol\,L^{-1}$ copper complex in the presence of $200\,\mu mol\,L^{-1}$ H_2O_2 and different amounts of Kojic acid.

3. Results and discussion

3.1. *IR and ^1H NMR spectroscopy of the ligands*

The ligands have been prepared using Fmoc as a protective group. Fmoc is generally removed from nitrogen of a peptide chain by acidolysis using trifluoroacetic acid (TFA) [19]. IR spectral data of MTS and CYS show two bands for $\nu(NH_2)$ (3348, 3260 cm^{-1}) for MTS and (3380, 3225 cm^{-1}) for CYS. The bands assigned to ν(NH) for MTS and CYS appear at 3100 and 3036 cm^{-1}, respectively. The two ligands also show bands attributed to ν(C=O), $\beta(NH_2)$, and ν(O=S=O) at 1650, 1494, and 1440 cm^{-1}, respectively [20, 21]. L-cystinoylsulfadiazine shows a weak band at 2600 cm^{-1} attributed to ν(S–H). ^{1}H NMR spectra of MTS and CYS in dimethyl-sulfoxide-d_6 exhibited signals at $\delta = 11.11$ and 11.26, respectively, assigned to 2 H, NH_2. L-cystinoylsulfadiazine shows a signal at $\delta = 2.08$ assigned to 1 H, SH. IR and ^{1}H NMR spectroscopies together with elemental analyses suggest the structure of the ligands as shown in schemes 1 and 2.

3.2. *IR spectroscopy of the copper(II) complexes*

To investigate the binding of copper to ligands, IR spectral data of the ligands were compared to that of the copper complexes. The bands attributed to $\nu(NH_2)$ in the IR spectrum of MTS ligand shift (3365, 3238 cm^{-1}) in Cu^{II}–MTS. The band attributed to $\beta(NH_2)$ shifts to 1504 cm^{-1} in the complex. The carbonyl ν(C=O) (at 1650 cm^{-1} in MTS) shifts to lower wavenumber (1632 cm^{-1}) in Cu^{II}–MTS with less intensity than that of the free ligand. Bands assigned to ν(O=S=O) and ν(NH) are unchanged, indicating no coordination. Spectral data show that copper(II) binds to the carbonyl oxygen and NH_2 nitrogen. Comparison of IR spectral data of CYS with its copper complex shows that the copper binds to the carbonyl oxygen and sulfur of deprotonated SH. This mode of binding was supported by disappearance of ν(SH) band in Cu^{II}–CYS spectrum as well as shifting of carbonyl to lower wavenumber (1634 cm^{-1}) with reduced intensity. There is no change in ν(NH), ν(O=S=O), and $\nu(NH_2)$, indicating no participation of these groups in binding. IR spectra show a broad band at ~3450 cm^{-1} assigned to ν(OH) in both copper(II) complexes.

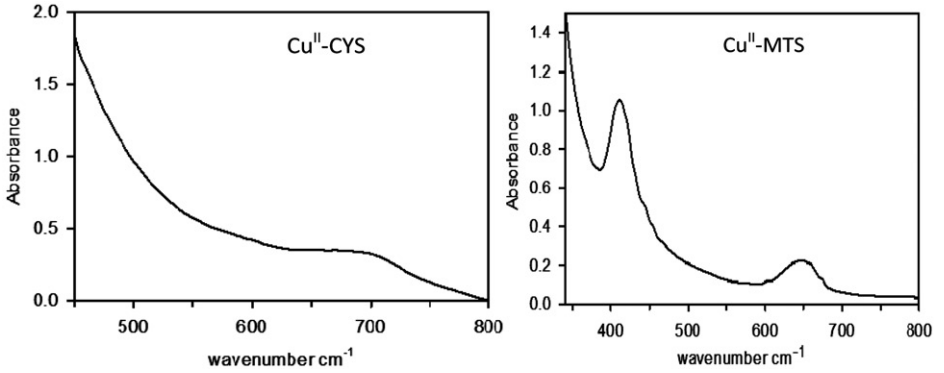

Figure 1. Electronic spectra of Cu^{II}–CYS and Cu^{II}–MTS complexes in DMSO.

3.3. *Electronic spectral data*

The magnetic moment (1.8 BM) of Cu^{II}–MTS at room temperature corresponds to one unpaired electron. Electronic spectrum of Cu^{II}–MTS in DMSO (figure 1) reveals absorption bands centered at 650 and 414 nm, attributed to d–d transition ($^2B_{1g} \rightarrow {}^2A_{1g}$) and charge transfer, respectively. These bands suggest square-planar geometry around copper [22]. The electronic spectrum of Cu^{II}–CYS in DMSO (figure 1) shows two bands at 270 and 320 nm, which can also be assigned to a CT band from filled orbitals of Cu(II) to the anti-bonding π^* orbitals of the CYS ligand [23]. In addition, a copper(II) complex with d^9 configuration is expected to experience Jahn–Teller distortion which leads to further splitting of the ^2E_g and $^2T_{2g}$ levels. Moreover, they give rise to the $^2B_{1g} \rightarrow {}^2A_{1g}$ (ν_1), $^2B_{2g}$ (ν_2), and ^2E_g (ν_3) transitions which are expected to be close in energy and generally appears as a broad band. Therefore the broad band centered at 700 nm is assigned to the envelope of $^2B_{1g} \rightarrow {}^2A_{1g}$, $^2B_{2g}$, and ^2E_g transitions [24] which support (with the magnetic moment = 1.9 BM) a distorted octahedral geometry around copper(II). The electronic spectral pattern exhibited by Cu^{II}–CYS in Nujol mull is similar to that obtained for the complex in DMSO, indicating that the geometry around the copper metal ion is likely to be the diaqua complex.

The EPR spectra of Cu^{II}–MTS and Cu^{II}–CYS were recorded as polycrystalline samples at room temperature and show hyperfine splitting, which indicates that there is an interaction between the metal center and the nitrogen adjacent to the copper(II). Both complexes exhibit an anisotropic signal. Analysis of the EPR spectral data (Supplementary material) gives $g_{\parallel} = (2.26499, 2.204911)$ and $g_{\perp} = (2.14629, 2.11621)$ for Cu^{II}–MTS and Cu^{II}–CYS, respectively. The $g_{\parallel} > g_{\perp} > 2.00$ indicate that the ground state of Cu(II) is predominately $d_{x^2-y^2}$ [25, 26]. The observed $g_{\parallel}$ values for Cu^{II}–MTS and Cu^{II}–CYS are less than 2.3, indicating that the bonds between ligand and copper have more covalent character than ionic. According to Hathaway and Billing [27], the magnitude of the ratio $G = (g_{\parallel} - 2)/(g_{\perp} - 2)$, which measures the exchange interaction between the copper centers in a polycrystalline solid, is 1.811 and 1.763 for Cu^{II}–MTS and Cu^{II}–CYS, respectively (G less than 4.0). This indicates considerable exchange interaction in the solid complex.

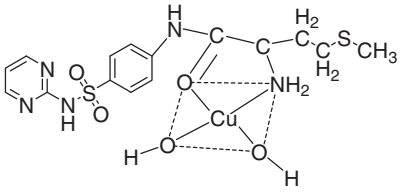

Scheme 3. Copper(II) complex of MTS, Cu^{II}–MTS.

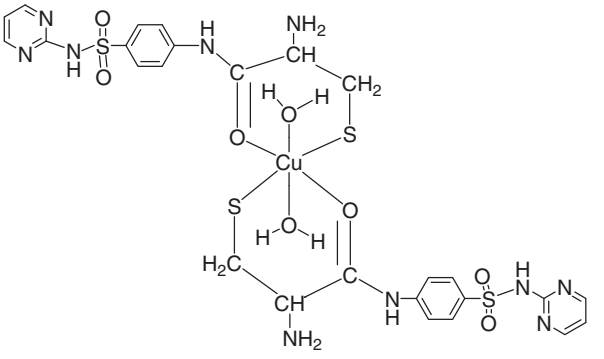

Scheme 4. Copper(II) complex of CYS, Cu^{II}–CYS.

3.4. *Thermal analysis*

The TGA confirms solvent inside and/or outside the coordination sphere and gives information about the stability of the compound. The thermogram of Cu^{II}–MTS (Supplementary material) shows four stages of mass loss from 25°C to 800°C. The first stage at 88°C corresponds to removal of one water molecule (Calcd = 3.7%, found = 3.0%). The second peak at 310°C corresponds to removal of NH_3, H_2O, CO_2, and C_2H_5–S–CH_3 (Calcd = 32.4%, found = 32.3%). The third stage at 470°C is assigned to $H_2NSO_2C_6H_4NH_2$ (Calcd = 36.0%, found = 36.3%). The TGA of Cu^{II}–CYS (Supplementary material) shows five inflections from 25°C to 800°C. The first stage at 135°C corresponds to removal of two water molecules (Calcd = 4.5%, found = 4.0%). The second stage at 210°C is assignable to two CH_3SH and one CO_2 (Calcd = 17.4%, found = 17.6%). The third and fourth stages together in the temperature range of 242.9–369.2°C correspond to two NH_3 and two CO_2 (Calcd = 15.2%, found = 15.2%). The weight loss (Calcd = 23.2%, found = 24.0%) in the fifth stage at 460°C is assigned to two $C_6H_5NH_2$.

The molar conductivities of Cu^{II}–MTS and Cu^{II}–CYS in DMSO at 25°C are 5 and 0 $\Omega^{-1}\,cm^2\,mol^{-1}$, respectively, indicating non-electrolytes [28]. The IR spectral data, electronic spectroscopy, EPR spectroscopy, thermal analysis, and elemental analysis support the structures for Cu^{II}–MTS and Cu^{II}–CYS (schemes 3 and 4).

3.5. *Molecular modeling*

For insight on the molecular structure of the preferred tautomers of ligand and complexes, the conformational analysis was performed. The computed molecular

Table 1. Calculated energies of keto and enol forms of MTS and Cu^{II}–MTS complex.

Method PM3	Keto	Enol	Complex
Heat of formation (kcal mol^{-1})	−46.238	−38.422	−243.18
Total energy (kcal mol^{-1})	−95,332.67	−95,324.86	−136,636.01
Binding energy (kcal mol^{-1})	−4476.00	−4468.18	−4924.86
HOMO (eV)	−9.20	−9.11	−9.00
LUMO (eV)	−9.21	−9.44	−7.00
Dipole (Debye)	3.58	7.908	8.76

Table 2. Calculated energies of keto and enol forms of CYS ligand.

Method PM3	Keto	Enol
Heat of formation (kcal mol^{-1})	−35.41	−27.101
Total energy (kcal mol^{-1})	−88,435.61	−88,427.3
Binding energy (kcal mol^{-1})	−3914.99	−3906.67
HOMO (eV)	−9.421	−9.34
LUMO (eV)	−9.44	−9.65
Dipole (Debye)	6.74	7.83

Table 3. Calculated energies of *cis* and *trans* isomeric forms of Cu^{II}–CYS.

Method PM3	*Cis*	*Trans*
Heat of formation (kcal mol^{-1})	710.06	426.42
Total energy (kcal mol^{-1})	−115,382.47	−206,638.33
Binding energy (kcal mol^{-1})	−6235.78	−6902.13
HOMO (eV)	−8.460	−8.55
LUMO (eV)	−7.25	−7.311
Dipole (Debye)	2.818	4.38

parameters, total energy, binding energy, heat of formation, the lowest unoccupied molecular orbital (LUMO), the highest occupied molecular orbital (HOMO) energies, and the dipole moment for studied compounds were calculated and presented in tables 1–3. Experimental determination of the tautomeric ligand structure is complicated and often unpredictable. The calculated molecular parameters have been used to investigate the most stable keto-enol isomer and showed that the most stable tautomer is keto for MTS and CYS. The optimized keto-enol tautomerization for MTS is illustrated in figure 2. Conjugation of the π-electrons of the carbonyl groups with the π-system of the molecular skeleton reduces the energy of the keto form, which leads to its predominance over the enol.

The possibility of existence of Cu^{II}–CYS in both *cis* and *trans* isomers was examined by calculating total energy, binding energy, heat of formation, LUMO, and HOMO energies (table 3). The most stable isomer is the *trans* (figure 3). The bond length between carbon and oxygen in the keto form of Cu^{II}–CYS was shorter than that in case of COH in the enol form. The CO and SH opposite to each other in the molecular skeleton lowered the energy of the *trans* isomer.

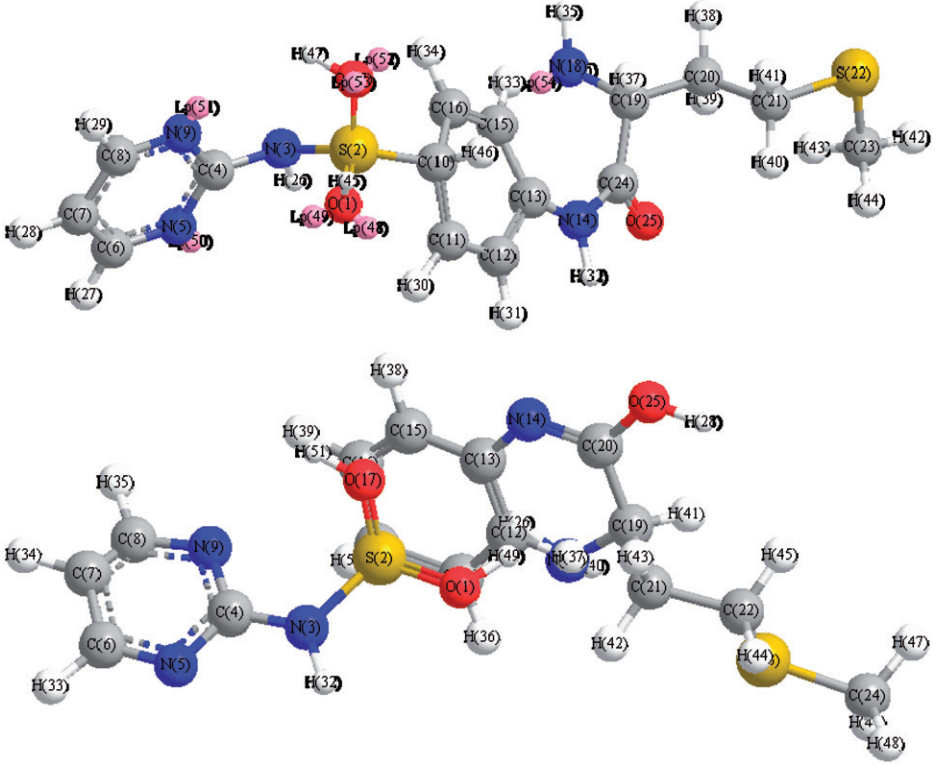

Figure 2. Ball and stick rendering for the keto and enol forms of MTS (from above to below, respectively), as calculated by PM3 semi-empirical molecular orbital calculations.

The bond length and bond angle for the keto and enol forms of the ligands together with the most stable complex isomer are calculated and listed in tables 1s–4s in "Supplementary material."

3.6. *Oxidation of phenol and catechol*

Although hydrogen peroxide has been used in oxidation of phenolic compounds, it requires additional activation by a catalyst for effective oxidation. Cu^{II}–MTS and Cu^{II}–CYS have been used in this study to activate H_2O_2 in oxidation of phenol and catechol. Phenol and catechol oxidations, which are very slow, are spectacularly enhanced by 100 μmol L^{-1} copper complex, reaching saturation at high concentration of the substrate. Such kinetic pattern indicates an enzyme-like pre-equilibrium kinetic pathway.

In order to study the catalytic activity of Cu^{II}–MTS and Cu^{II}–CYS and their interaction with H_2O_2 toward oxidation of phenolic compounds, phenol and catechol have been used as substrates to provide detailed kinetic information. The oxidation rates of phenol by 100 μmol L^{-1} Cu^{II}–MTS and 100 μmol L^{-1} Cu^{II}–CYS at different concentrations of phenol (figure 4) have been determined in the presence of

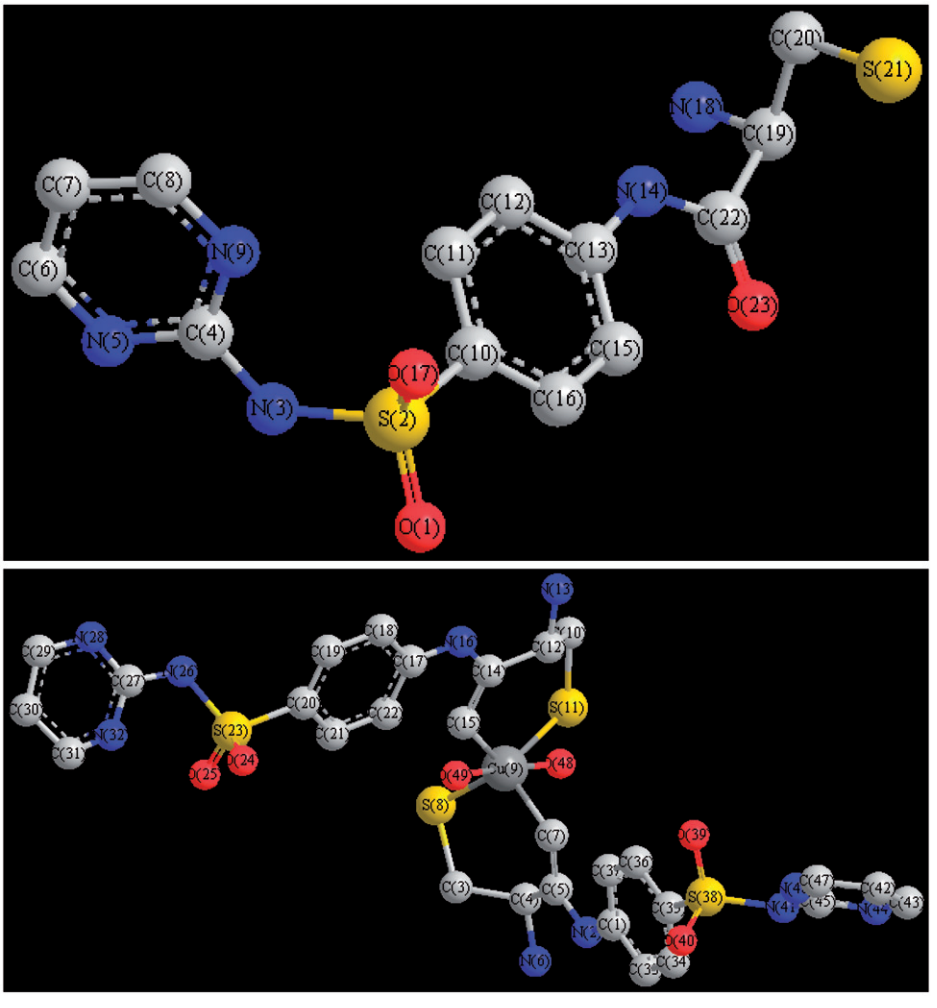

Figure 3. Ball and stick rendering for the most stable tautomer form of CYS (keto form) and *trans* isomer of its complex (from top to bottom, respectively; hydrogen atoms were removed for clarity), as calculated by PM3 semi-empirical molecular orbital calculations.

200 μmol L^{-1} H_2O_2 at room temperature. The rate of phenol oxidation using either Cu^{II}–MTS or Cu^{II}–CYS is nonlinear, reaching saturation at high substrate concentrations which suggests enzyme-like pre-equilibrium kinetics. This kinetics can be described as the binding of the substrate (S = phenol) with the catalyst to form an intermediate S–Cu^{II}-complex, followed by conversion of the bound substrate into products (equation (1)).

$$Cu^{II}\text{-complex} + S \underset{k_{-1}}{\overset{k_1}{\rightleftharpoons}} Cu^{II}\text{-complex-S} \xrightarrow{k_{cat}} Cu^{II}\text{-complex} + \text{Prod.} \qquad (1)$$

where Cu^{II}-complex = Cu^{II}-MTS or Cu^{II}-CYS, S = phenol or catechol.

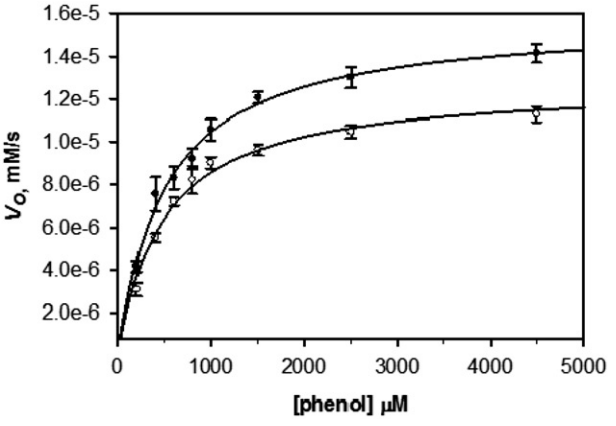

Figure 4. Oxidation of phenol using 100 μmol L^{-1} of Cu^{II}–MTS (•) and 100 μmol L^{-1} Cu^{II}–CYS (○) in the presence of 200 μmol L^{-1} H_2O_2 at 25°C.

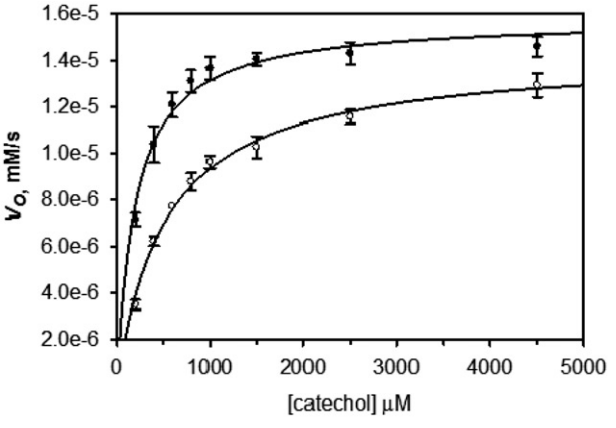

Figure 5. Oxidation of catechol using 100 μmol L^{-1} Cu^{II}–MTS (•) and 100 μmol L^{-1} Cu^{II}–CYS (○) in the presence of 200 μmol L^{-1} H_2O_2 at 25°C.

The rate law for this reaction can be obtained with steady-state approximation similar to the Michaelis–Menten kinetics in enzyme catalysis and can be expressed as in equation (2),

$$\text{Rate} = \frac{k_{\text{cat}}[\text{Cu}^{\text{II}}\text{-complex}][\text{S}]}{K' + [\text{S}]} \tag{2}$$

where $K' = (k_{-1} + k_{\text{cat}})/k_1$ is the dissociation constant of the S–Cu^{II}-complex. This reaction produces a first-order rate constant $k_{\text{cat}} = 1.58 \times 10^{-2}\,\text{s}^{-1}$ ($t_{1/2} = 43.9$ s) for Cu^{II}–MTS and $k_{\text{cat}} = 1.27 \times 10^{-2}\,\text{s}^{-1}$ ($t_{1/2} = 54.6$ s) for Cu^{II}–CYS. Oxidation of 1.0 mmol L^{-1} of phenol or catechol using 100 μmol L^{-1} Cu^{II}–MTS in the absence of H_2O_2 affords k_{cat} of $1.40 \times 10^{-5}\,\text{s}^{-1}$ and $1.42 \times 10^{-5}\,\text{s}^{-1}$, respectively. Oxidation of catechol using 100 μmol L^{-1} Cu^{II}–MTS or 100 μmol L^{-1} Cu^{II}–CYS in the presence of 200 μmol L^{-1} H_2O_2 (figure 5) is similar to phenol oxidation with the saturation

Table 4. Oxidation of phenol and catechol using Cu^{II}–MTS and Cu^{II}–CYS in the presence of H_2O_2 at room temperature.

Catalyst	Substrate	k_{cat} (s^{-1})	K' (mmol L^{-1})	$t_{1/2}$ (s)	C.P.	k_{cat}/K' (mol $L^{-1})^{-1}$ s^{-1}
Cu^{II}–MTS	Phenol	1.58×10^{-2}	0.51	43.87	3.43×10^5	30.98
Cu^{II}–CYS	Phenol	1.27×10^{-2}	0.48	54.57	2.77×10^5	26.45
Cu^{II}–MTS	Catechol	1.58×10^{-2}	0.21	43.87	3.34×10^4	75.23
Cu^{II}–CYS	Catechol	1.43×10^{-2}	0.53	48.47	3.02×10^4	26.98
Cu^{II}–MTS	H_2O_2	1.83×10^{-2}	0.42	37.87	3.98×10^5	43.57
Cu^{II}–CYS	H_2O_2	1.60×10^{-2}	0.43	43.32	3.49×10^5	37.20

C.P. = catalytic proficiency.

pattern to produce first-order rate constant $k_{cat} = 1.58 \times 10^{-2}\,s^{-1}$ ($t_{1/2} = 43.9$ s) for Cu^{II}–MTS and $k_{cat} = 1.43 \times 10^{-2}\,s^{-1}$ ($t_{1/2} = 48.5$ s) for Cu^{II}–CYS. The dissociation constants K' were also obtained and are listed in table 4. Free-radical initiated oxidation would not show such pre-equilibrium kinetics and the substrate bound intermediate [29]. To investigate the existence of free radical in the reaction mechanism, various concentrations of $(CH_3)_2SO$ were used in oxidation of 1.0 mmol L^{-1} phenol or catechol in the presence of H_2O_2 using Cu^{II}–MTS and Cu^{II}–CYS. The free radical scavenger $(CH_3)_2SO$ [30] did not inhibit the reaction, suggesting the absence of free radical to induce the oxidation reaction.

The complexes show significant catalytic efficiency k_{cat}/K' (table 4). The catalytic activity of Cu^{II}–MTS toward oxidation of phenol shows $k_{cat}/K' = 30.98$ (mol $L^{-1})^{-1}s^{-1}$ as the second-order rate constant. Moreover, the catalysis shows 3.43×10^5 times rate enhancement in terms of the first-order rate constant (k_{cat}/k_o, wherein $k_o = 4.6 \times 10^{-8}\,s^{-1}$ is the rate constant for the uncatalyzed phenol oxidation). Catalytic activity of catechol oxidation using Cu^{II}–MTS is 75.23 (mol $L^{-1})^{-1}$ s^{-1} as the second-order rate constant, showing 3.34×10^4 rate enhancement in terms of first-order rate constant compared to uncatalyzed catechol oxidation reaction $k_o = 4.74 \times 10^{-7}\,s^{-1}$. Table 4 shows that the copper complex of methionionylsulfadiazine (Cu^{II}–MTS) is more active in oxidation of either phenol or catechol in the presence of H_2O_2 at room temperature than Cu^{II}–CYS. This activity may be due to different geometries around Cu(II) in the two complexes. The square-planar Cu^{II}–MTS leaves two positions free around copper, which may facilitate the binding of the substrate to the metal ion or forming OH bridge. The octahedral geometry in Cu^{II}–CYS occupies all six coordination sites around copper, slowing the binding of the substrate to copper. Oxidation of phenol and catechol using the copper complexes as a function of H_2O_2 also shows a saturation pattern at high concentrations of H_2O_2 (figure 6), indicating direct binding of this oxidant as a substrate to the active metal center. Both substrates bind to the enzyme model to produce a ternary complex [18, 31, 32]. The order of binding can either be random (in a random mechanism) or substrates have to bind in a particular sequence (in an ordered mechanism). The kinetics indicates that H_2O_2 can bind to (Cu-complex) to form a ternary complex H_2O_2–(Cu-complex)–(cat. or ph) [31]. The first-order rate constants k_{cat}, $t_{1/2}$, and catalytic activity are listed in table 4. The rate constants in the studies herein are comparable or higher than those of a number of structurally defined Cu^{II}-complexes toward oxidation of catechol. For example, k_{cat} for the oxidation of catechol is in the range $(1.6–2.2) \times 10^{-4}\,s^{-1}$ by Cu^{II}-macrocycle complexes [33] and $(2.75–5.13) \times 10^{-4}\,s^{-1}$ and $(3.98–13.2) \times 10^{-3}\,s^{-1}$ by some dinuclear Cu^{II}-complexes

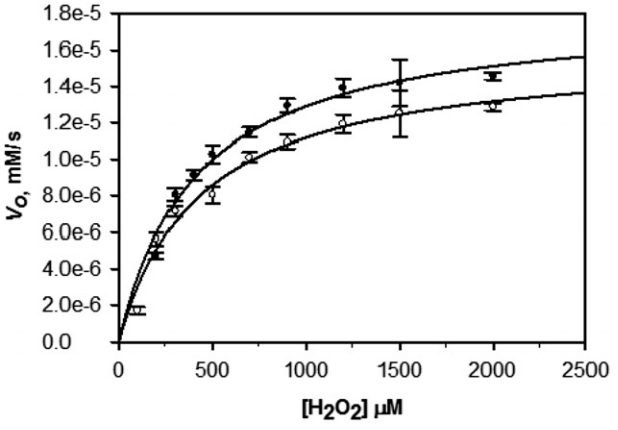

Figure 6. Oxidation of phenol using 100 μmol L^{-1} Cu^{II}–MTS (•) and 100 μmol L^{-1} Cu^{II}–CYS (○) in the presence of different concentrations of H_2O_2 at 25°C.

[34, 35]. The Cu^{II}–MTS and Cu^{II}–CYS complexes showed $k_{cat} = \sim 6.2 \times 10^3$ and 1.1×10^3 times more toward oxidation of catechol than copper(II)-(4-vinylbenzyl) cytosine ($k_{cat} = 2.53 \times 10^{-6}\,s^{-1}$) [36] and copper-metallated nucleobase polymeric matrix (9-allyladenine-1,4-divinylbenzene cross polymer) (1.32×10^{-5} s^{-1}) [37]. The rate constants herein are only about 8 times lower than that of the Cu^{II}-complex of a vinylpyridine-acrylamide copolymer ($k_{cat} = 0.12\,s^{-1}$) [32]. Oxidation of catechol using Cu^{II}–MTS and Cu^{II}–CYS showed $k_{cat} \sim 3.1 \times 10^3$ and 1.3×10^4 times more than that of oxidation of 4-*t*-butylcatechol ($k_{cat} = 4.65 \times 10^{-6}\,s^{-1}$ and $1.15 \times 10^{-6}\,s^{-1}$) [36, 37]. The first-order rate constants of phenol oxidation using Cu^{II}–MTS and Cu^{II}–CYS are only about 13–16 times lower than that of Cu^{II}-β amyloid1-20 ($k_{cat} = 0.213\,s^{-1}$) [38].

To investigate the effect of the catalyst concentration on oxidation of phenol, different concentrations of Cu^{II}–MTS were used in oxidation of 1.0 mmol L^{-1} phenol in the presence of 200 μmol L^{-1} H_2O_2 at room temperature. The observed rate was linear till ~100 μmol L^{-1} of copper complex and then reached saturation (figure 7), indicating that the optimum concentration for the copper complex is 100 μmol L^{-1}. The same concentration has been used in Cu^{II}–CYS for data comparison.

3.7. *Inhibition of phenol and catechol oxidation by Kojic acid*

Kojic acid, which has a quinoid structure, can act as a tyrosinase inhibitor (to inhibit melanin formation) and as antioxidant for fats and oils in cosmetics (skin whitening or depigmenting agent). Applications also include the prevention of discoloration of crustacea, meat, and fresh vegetables. In this study, Kojic acid was used to inhibit the Cu^{II}–MTS complex toward oxidation of both phenol and catechol. Figure 8 shows that both phenol and catechol oxidation is inhibited significantly by Kojic acid with IC_{50} ~100 and ~95 μmol L^{-1} for phenol and catechol, respectively. Phenol oxidation has been inhibited by Kojic acid using Cu^{II}–CYS, showing no big change for Cu^{II}–CYS rather than using Cu^{II}–MTS.

These copper(II) complexes can be used as an oxidative model to discover new inhibitors that can be used in the cosmetic and medicinal products used to prevent

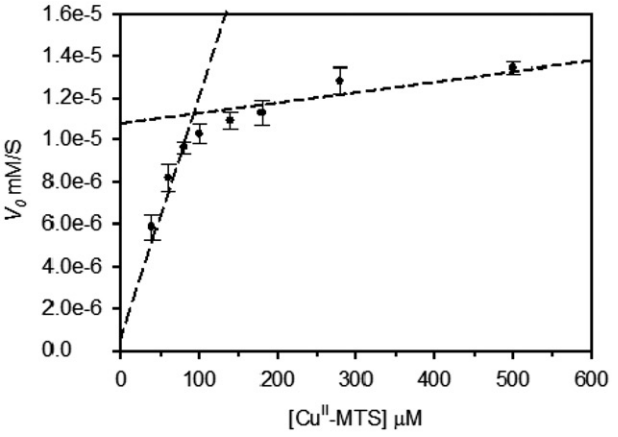

Figure 7. Oxidation of phenol using different concentrations of Cu^{II}–MTS in the presence of 200 μmol L^{-1} H_2O_2 at 25°C.

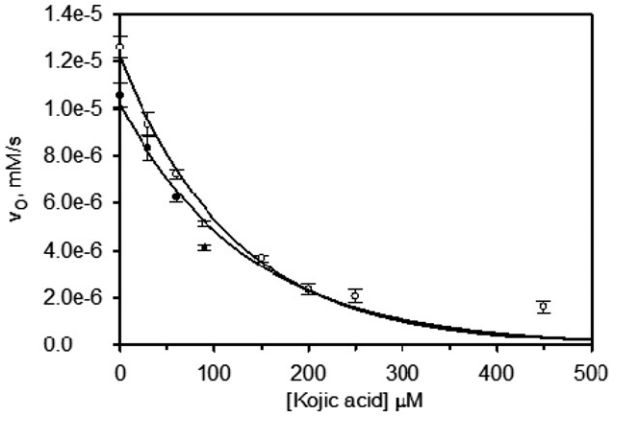

Figure 8. Inhibition of phenol oxidation (•) and catechol oxidation (○) using different concentrations of Kojic acid by 100 μmol L^{-1} Cu^{II}–MTS in the presence of 200 μmol L^{-1} H_2O_2 at 25°C.

hyperpigmentation [39]. Moreover, these inhibitors can be used as antioxidants and anticancer agents.

4. Conclusion

We have prepared new copper(II) complexes of sulfadiazine with DL-methionine and L-cystine amino acids. These complexes can be used as environmentally acceptable catalysts due to the presence of antimicrobial sulfadiazine and amino acids. The keto form was predominant over enol. Cu^{II}–MTS and Cu^{II}–CYS can promote the oxidation

of phenol and catechol in the presence of the green oxidizing agent H_2O_2. The rate constants are comparable or higher than those published. Cu^{II}–MTS is more active in the oxidation of phenol or catechol than Cu^{II}–CYS, due to the octahedral geometry around copper in Cu^{II}–CYS. The copper(II) complexes provide model systems for further investigation of Cu-centered oxidation and oxygenation chemistry.

Acknowledgments

The authors acknowledge Taif University for supporting this work by Taif University research program (2-432-711).

References

[1] C. Gerdeman, C. Eicken, B. Krebs. *Acc. Chem. Res.*, **35**, 183 (2002).
[2] A. Rompel, C. Gerdemann, A. Vogel, B. Krebs. *Inorganic Chemistry Highlights*, Wiley VCH-Verlag, Weinheim, Germany (2002).
[3] E.J. Land, C.A. Ramsden, P.A. Riley. *Acc. Chem. Res.*, **36**, 300 (2003).
[4] E.A. Lewis, W.B. Tolman. *Chem. Rev.*, **104**, 1047 (2004).
[5] I. Bouabdallah, R. Touzani, I. Zidane, A. Ramdani. *J. Iran. Chem. Soc.*, **4**, 299 (2007).
[6] E. Monzani, L. Quinti, A. Perotti, L. Casella, M. Gullotti, L. Randaccio, S. Geremia, G. Nardin, P. Faleschini, G. Tabbi. *Inorg. Chem.*, **37**, 553 (1998).
[7] L.Q. Hatcher, K.D. Karlin. *J. Biol. Inorg. Chem.*, **9**, 669 (2004).
[8] P. Gentschev, N. Möller, B. Krebs. *Inorg. Chim. Acta*, **300–302**, 442 (2000).
[9] C. Fernandes, A. Neves, A.J. Bortoluzzi, A.S. Mangrich, E. Rentschler, B. Szpoganicz, E. Schwingel. *Inorg. Chim. Acta*, **320**, 12 (2001).
[10] M.R. Malachowski, J. Carden, M.G. Davidson, W.L. Driessen, J. Reedijk. *Inorg. Chim. Acta*, **257**, 59 (1997).
[11] S. Yamada. *Coord. Chem. Rev.*, **190–192**, 537 (1999).
[12] I.A. Koval, P. Gamez, C. Belle, K. Selmeczi, J. Reedijk. *Chem. Soc. Rev.*, **35**, 814 (2006).
[13] V. Mahadevan, R.J.M. Klein Gebbink, T.D.P. Stack. *Curr. Opin. Chem. Biol.*, **4**, 228 (2000).
[14] L.I. Simandi. *Catalytic Activation of Dioxygen by Metal Complexes*, Kluwer Academic Publishers, Dordrecht (1992).
[15] J. Reedijk (Ed.). *Bioinorganic Catalysis*, Marcel Dekker, New York (1993).
[16] S. Profeta, N.L. Allinger. *J. Am. Chem. Soc.*, **107**, 1907 (1985).
[17] J.J.P. Stewart. *J. Comput. Chem.*, **10**, 221 (1989).
[18] G.F.Z. da Silva, W.M. Tay, L.J. Ming. *J. Biol. Chem.*, **280**, 16601 (2005).
[19] E. Wünsch, E. Jaeger, L. Kisfaludy, M. Löw. *Angew. Chem.*, **16**, 317 (1977).
[20] H.Y. Mostafa. *J. Pigment & Resin. Res. Tech.*, **35**, 71 (2006).
[21] P. Selvam, P. Rathore, S. Karthikumar, K. Velkumar, P. Palanisamy, S. Vijayalakhsmi, M. Witvrouw. *Ind. J. Pharm. Sci.*, **71**, 432 (2009).
[22] T. Ahamad, N. Nishat. *J. Appl. Polym. Sci.*, **107**, 2280 (2008).
[23] C. Fraser, B. Bosnich. *Inorg. Chem.*, **33**, 338 (1994).
[24] R. Li, B. Moubaraki, K.S. Murray, S. Brooker. *Dalton Trans.*, 6014 (2008).
[25] T. Ahamad, V. Kumar, S. Parveen, N. Nishat. *J. Coord. Chem.*, **61**, 1423 (2008).
[26] N. Nishat, T. Ahamad, S.M. Alshehri, S. Parveen. *Eur. J. Med. Chem.*, **45**, 1287 (2010).
[27] B.J. Hathaway, D.E. Billing. *Coord. Chem. Rev.*, **5**, 143 (1970).
[28] W.J. Geary. *Coord. Chem. Rev.*, **7**, 81 (1971).
[29] J.A. Zazo, J.A. Casas, A.F. Mohedano, M.A. Gilarranz. *J. Environ. Sci. Technol.*, **39**, 9295 (2005).
[30] P.S. Rao, J.M. Luber, J. Milinowicz, P. Lalezari, H.S. Mueller. *Biochem. Biophys. Res. Commun.*, **150**, 39 (1988).
[31] W.M. Tay, A.I. Hanafy, A. Angerhofer, L.J. Ming. *Bioorg. Med. Chem. Lett.*, **19**, 6709 (2009).
[32] V. Lykourinou, A.I. Hanafy, G.F.Z. da Silva, K.S. Bisht, R.W. Larsen, B.T. Livingston, A. Angerhofer, L.J. Ming. *Eur. J. Inorg. Chem.*, 2584 (2008).

[33] N. Sengottuvelan, D. Saravanakumar, V. Narayanan, M. Kandaswamy, K. Chinnakali, G. Senthilkumar. *Bull. Chem. Soc. Japan*, **77**, 1153 (2004).
[34] P. Akilan, M. Thirumavalavan, M. Kandaswamy. *Polyhedron*, **22**, 3483 (2003).
[35] S.C. Cheng, H.H. Wei. *Inorg. Chim. Acta*, **340**, 105 (2002).
[36] C.S. Purohit, M. Parvez, S. Verma. *Appl. Catal., A*, **316**, 100 (2007).
[37] S.G. Srivatsan, Poonam Nigam, M.S. Rao, Sandeep Verma. *Appl. Catal., A*, **209**, 327 (2001).
[38] G.F.Z. da Silva, L.J. Ming. *Angew. Chem. Int. Ed.*, **44**, 5501 (2005).
[39] A.A. Bell, M.H. Wheeler. *Annu. Rev. Phytopathol.*, **24**, 411 (1986).